Water Air Soil Pollut (2024) 235:748
https://doi.org/10.1007/s11270-024-07564-w

Check for updates

Emission Factors, Chemical Composition and Ecotoxicity of PM_{10} from Road Dust Resuspension in a Small Inland City

Yago Alonso Cipoli · Ismael Casotti Rienda · Ana M. Sánchez de la Campa · Nora Kováts · Teresa Nunes · Manuel Feliciano · András Hoffer · Beatrix Jancsek-Turóczi · Célia Alves

Received: 5 July 2024 / Accepted: 8 October 2024 / Published online: 15 October 2024

Abstract Road dust resuspension in urban environments can contribute to high human exposure to metal(loid)s, polycyclic aromatic hydrocarbons, and other potentially toxic organic compounds. However, for many regions, information on loadings, emission factors and chemical profiles is lacking to accurately apply emission inventories and source apportionment models. In the present study, PM_{10} samples were collected with an in situ road dust sampler from eleven representative streets of Bragança, an inland city of the Iberian Peninsula, and were analysed for organic and elemental carbon by a thermal-optical technique, elemental composition by ICP-MS and ICP-OES, and ecotoxicity by a luminescence inhibition bioassay with *Allivibrio fischeri*. A global emission factor of 5.36 ± 2.35 mg veh^{-1} km^{-1} was obtained but in suburban areas the values reached twice the average. Total carbon accounted for $14.9 \pm 6.8\%$ of the PM_{10} mass, while element oxides represented the largest share ($28.6 \pm 18.7\%$). Very high enrichments were found for typical traffic-related elements such as Cu, Zn, S, Pb and Ni. The geochemical index I_{geo} further confirmed that road dust of the study region is extremely contaminated by elements mainly originated from tyre and brake wear. Although the total non-carcinogenic and carcinogenic risks associated with metal exposure were found to be low for both children and adults, the bioluminescence inhibition assay showed (eco)toxic

Highlights
- The PM_{10} fraction of road dust was sampled with a mobile resuspension chamber.
- Emission factors were lower than in other cities.
- Road dust was highly contaminated by elements from brake and tyre wear.
- Cancer and non-cancer risks from exposure to metals were low.
- All samples proved to be (eco)toxic.

Supplementary Information The online version contains supplementary material available at https://doi.org/10.1007/s11270-024-07564-w.

Y. A. Cipoli (✉) · I. C. Rienda · T. Nunes · C. Alves (✉)
Centre for Environmental and Marine Studies (CESAM), Department of Environment, University of Aveiro, 3810-193 Aveiro, Portugal
e-mail: yagocipoli@ua.pt

C. Alves
e-mail: celia.alves@ua.pt

A. M. S. de la Campa
Center for Research in Sustainable Chemistry-CIQSO, Associate Unit CSIC-University of Huelva "Atmospheric Pollution", Campus El Carmen S/N, 21071 Huelva, Spain

A. M. S. de la Campa
Department of Mining, Mechanic, Energetic and Construction Engineering, ETSI, University of Huelva, 21071 Huelva, Spain

N. Kováts
Centre of Natural Environmental Sciences, University of Pannonia, Egyetem Str. 10, 8200 Veszprém, Hungary

M. Feliciano
Centro de Investigação de Montanha (CIMO), Instituto Politécnico de Bragança, 5300-253 Bragança, Portugal

responses for all samples, indicating that road dust resuspension may pose a significant human health and ecological threat.

Keywords Road dust · PM_{10} · Emission factors · Chemical profiles · Health risks · Toxicity

1 Introduction

Air pollution is one of main risk factors for public health and a global concern (Duan et al., 2020). A recent global exposure mortality model estimated that the annual excess mortality rate from ambient air pollution in Europe (EU-28) is 790,000, mainly due to cardiovascular events (Lelieveld et al., 2019). Particulate matter is one of the most dangerous air pollutants. More than 90% of the global population lives in areas where particulate matter with aerodynamic diameter of less than 2.5 µm ($PM_{2.5}$) exceeds the World Health Organisation air quality guidelines of 10 µg m^3 annual mean (WHO AQGs) (Shaddick et al., 2020). Exposure to ambient PM air pollution is a major risk of premature death (Apte et al., 2018). In urban areas, traffic-related emissions are often pointed out as the main and predominant source of particulate matter (Casotti Rienda & Alves, 2021; EEA, 2020). Over the past decade there have been significant developments and improvements in air quality and reductions in road vehicle emissions have been a major contributor to this trend (Harrison et al., 2021a, 2021b). However, emissions from the road traffic sector still represent an appreciable contribution to global air pollution, including not only tailpipe emissions, which have been gradually reduced, but also the so-called non-exhaust emissions, which require other control measures (Padoan & Amato, 2018). Non-exhaust emissions comprise mainly four different processes: brake wear, road surface wear, tyre wear and road dust resuspension. Road dust resuspension arises from any particle on road surface that becomes suspended in the air by passing traffic and wind (Harrison et al., 2021a, 2021b). Unlike exhaust emissions, non-exhaust emissions are not subject to specific legislative control currently.

Road dust composition and loadings vary depending on the state of the road surface (Alves et al., 2018), type of pavement (Gustafsson et al., 2019), traffic patterns (Farwick zum Hagen et al., 2019), wetness conditions (Hicks et al., 2021) and the processes governing dust removal from the road surface. A literature review by Casotti Rienda and Alves (2021) showed that road dust can be enriched with metals, metalloids and polycyclic aromatic hydrocarbons (PAHs) of human health concern. Furthermore, the same authors also reported that, nowadays, non-exhaust emissions of particulate matter account for up to 90% by mass of total PM emitted by traffic. In turn, road dust resuspension can represent a share of 28–59% of PM_{10} from non-exhaust sources, varying with local conditions. To more accurately apply emission inventories and source assignment receptor models, locally obtained dust loadings, emission factors and chemical profiles should be used.

In Portugal, detailed information on the chemical composition of resuspended road dust from the coastal cities of Oporto (Alves et al., 2018), Viana do Castelo (Célia A. Alves et al., 2020; Candeias et al., 2020), Aveiro (Casotti Rienda et al., 2023a, 2023b) and Lisbon (Cunha-Lopes et al., 2022) has been documented. Like other studies reported in Europe, the focus has been on medium-large urban centres (Casotti Rienda & Alves, 2021). The purpose of this study is to complement the previous ones by providing PM_{10} road dust detailed information for Bragança, a small inland city in Portugal. Near Bragança, the main activity and land use is related to agricultural smallholdings, while the urban centre has a weak industrial activity, with a dominance of the commercial sector. Therefore, this work aimed to provide dust loadings, chemical composition, and toxicity of PM_{10} from road dust resuspension for a city with an economic fabric, weather patterns and topography different from the previous ones, but which represents the characteristics of other inland municipalities in the Iberian Peninsula or even in other regions of Europe. The proposed methodology seeks to provide useful information to national and international emission inventories, chemical profile repositories and policy makers, so that the databases can be used for more

M. Feliciano
Laboratório Associado Para a Sustentabilidade E Tecnologia Em Regiões de Montanha (SusTEC), Instituto Politécnico de Bragança, 5300-253 Bragança, Portugal

A. Hoffer · B. Jancsek-Turóczi
HUN-REN–PE Air Chemistry Research Group, 8200 Veszprém, Hungary

realistic simulations and to support decision making to improve air quality.

2 Material and Methods

2.1 Study Area and Monitored Sites

Bragança is in the extreme northeast of mainland Portugal, at 650–700 m above sea level. The city is in a mountainous region with a complex relief (Gonçalves et al., 2018). The climate is characterised by high annual and monthly thermal amplitude, with dry and hot summers and frequent rains in winter. The area of Bragança holds indeed an economic structure composed by diverse urban fabric, mainly related to commercial and agricultural activities. Several villages and agricultural areas are also located in the surrounding region. A significant number of potential air contamination sources are present within and around this urbanised area, especially exhaust and non-exhaust traffic emissions, and biomass burning (mainly in the cold season) (Cipoli et al., 2023).

In this source-oriented study, field sampling was carried out in July 2024 within the area delimited by the municipality of Bragança. The road segments were selected in collaboration with the city council taking into consideration traffic densities, urban structures, and paved streets. In the end, eleven different road segments were selected (Fig. 1).

The sampling sites comprised different land-uses, including:

- Suburban context (RD1, RD2, RD5 and RD11) – Roads with rather deteriorated pavement on the outskirts of the city with a low traffic density. One side of the street usually consists of dispersed detached houses, while the other side is surrounded by farms.
- Industrial context (RD3) – Road within the industrial area, surrounded by service and commercial buildings. This area is characterised by the high frequency of heavy-duty vehicles (Cipoli et al., 2022), with pavement in good conditions.
- Urban context (RD4) – Avenue located around the campus of the Polytechnic University of Bragança with connection to the city centre. It is an avenue with residential neighbourhoods, shops, services, and bike/walk lanes.
- Urban context (RD6 and RD7) – Roads located within residential areas, flanked by semi-detached houses, with low traffic intensity.
- Urban context (RD8) – Segment in the main avenue of the city, with high density of vehicles, located 500 m from a tunnel and surrounded by buildings on both sides of the street (low height urban canyon).

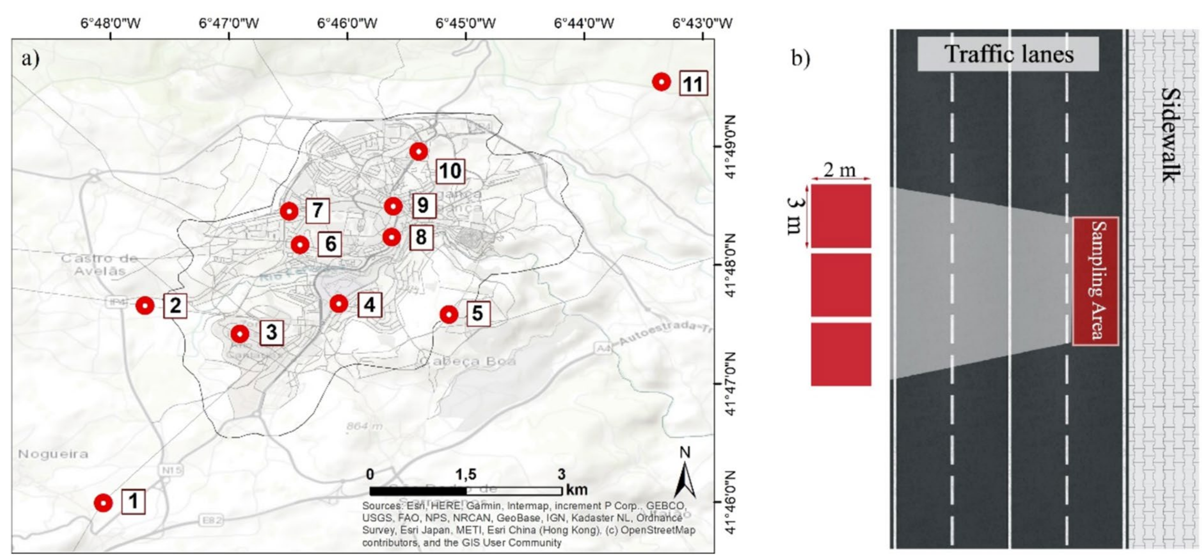

Fig. 1 **a** Location of monitored streets in the municipality of Bragança, and **b**) road sampling configuration

- Urban context (RD9) – Segment in a 235 m long tunnel.
- Urban context (RD10)—Segment located 300 m from the tunnel, on the city's main avenue. One side of the avenue is surrounded by Braguinha Park, a green area widely used for sports and recreation. The other side of the avenue is characterised by a vacant lot.

The pavement of urban streets was, in general, in good condition due to regular maintenance and conservation.

2.2 Road Dust Sampling and Experimental Set-up

A total of 33 dust samples were collected from delimited paved road segments after a weeklong of dry period without any wet weather event. Samples were collected during the central hours of the day, usually from 10 a.m. to 5 p.m., to avoid moisture condensation on roads. For each sampling site, 3 replicates, two on quartz filters and one on Teflon filters, were collected to enhance the representativeness of results. The segments were on the right side of the right lane. Three spots of 2.0 m×3.0 m were selected in an attempt of encompassing road dust resuspension particles from pavement abrasion, tyre and brake wear, and sedimented material from other sources in the vicinities. The PM_{10} samples were collected with a mobile resuspension road dust sampler (Fig. 2), first developed by Jancsek-Turóczi et al. (2013).

This device induces resuspension and collects particles directly from road surfaces. Particles are resuspended in a rectangular stainless-steel hood that is attached to the front of a cart at 0.5 cm from the pavement. A leaf blower (Makita UB1101, 600 W) was connected to the hood through two facing nozzles via a split flexible hose, designed to induce turbulence and resuspend road dust from solid surfaces. A low-volume sampler (Echo PM TECORA, Italy) was mounted on the cart and connected to the hood with a stainless-steel tube. The low-volume sampler collected resuspended PM_{10} on pre-weighed 47 mm in diameter quartz fibre or Teflon filters, both from Pall. Each filter was sampled for 40 min, covering an area of 6 m^2. This sampler has already been used to collect road dust in Hungary and more details and specifications of the equipment assembly can be found in Jancsek-Turóczi et al. (2013). The equipment used is suitable for sampling during dry periods. Sampling on humid or wet pavements would contribute to the breakdown of filters and electrical failures in the equipment. Winters in Bragança are characterised by recurrent rains and high humidity, which would prevent the use of the equipment. However, other studies have demonstrated seasonal variations of dust loadings as well as chemical composition between winter and summer months (Gulia et al., 2019; Han et al.,

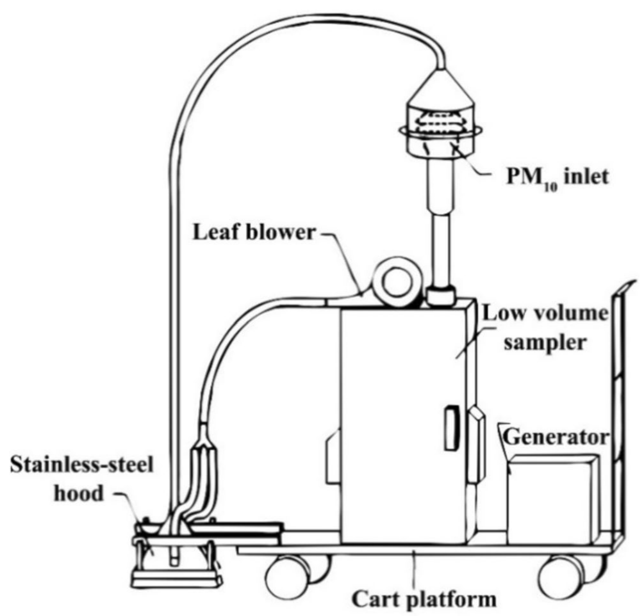

Fig. 2 Schematic representation of the mobile resuspended PM_{10} sampling unit. Adapted from Jancsek-Turóczi et al. (2013)

2007), mostly related to the washout effect of rain and to higher humidity at the level of the pavement surface (Amato et al., 2011).

2.3 Laboratory Procedures and Physico-Chemical Determinations

The preparation of quartz filters prior to measurements involved calcination at 500 °C for 6 h to remove any potential organic contaminants. Before weighting, both quartz and Teflon filters were stabilised for 48–72 h under controlled conditions of temperature at 20 °C and 50% relative humidity, in accordance with the European Standard EN 12341 (Ambient air—Standard gravimetric measurement method for the determination of the PM_{10} mass concentration). Gravimetric quantifications were performed using a Radwag 5/2Y/F microbalance (accuracy of 1 µg). After gravimetric determination, samples were stored in a freezer at − 20 °C until further processing.

2.4 Carbonaceous Content

Two replicate analyses of the carbonaceous content (organic (OC) and elemental carbon (EC), of PM_{10} collected on quartz filters was performed by a thermal optical transmission technique. Circular punches of 9 mm were subjected to a controlled heating process with a sequence of temperature steps overtime following the EUSAAR-2 protocol. In the first minutes, OC is volatilised in an inert atmosphere of nitrogen, and afterwards in an oxidising atmosphere (4% oxygen-rich O_2/N_2) to determine the EC. Light transmittance is measured by a laser beam and photodetector, which allows to separate the EC formed during pyrolysis of OC from the EC originally present in the sample. Details on how the system works and the complete methodology are described elsewhere (Alves et al., 2011; Pio et al., 2011).

2.5 Major and Trace Elements

Teflon filters were instead fully allocated to the determination of major and trace elements. Filters were acid digested for the analysis of major elements by inductively coupled plasma-optical emission spectrometry (ICP-OES; Agilent model 5110) and trace elements by inductively coupled plasma mass spectroscopy (ICP-MS; Agilent model 7900). For quality control, the analytical procedure was validated during the run of both ICP instruments using the NIST-1633c fly ash reference standard material. External calibrations were made using elemental standard solutions. More details about the procedures can be found in Millán-Martínez et al. (2021).

2.6 Ecotoxicity Assessment

The ecotoxicity potential of PM_{10} samples was determined by the bioluminescence inhibition bioassay of the *Aliivibrio fischeri* bacterium. When exposed to toxic compounds, this organism shows a decrease in its luminous emittance (Kováts & Horváth, 2016). The protocol follows the ISO standard 21338:2010 (water quality kinetic determination of the inhibitory effects of sediment, other solids, and coloured samples on the light emission of *V. fischeri*/kinetic luminescent bacteria test), and the experimental protocol developed by Kováts et al. (2012). To identify stressor-response patterns, one portion of the quartz filters was water-extracted and several dilutions were prepared. The direct contact test was made in a double measurement of bioluminescence: the first one happening 30 s after exposure to the bacterial suspension, and the second one after 30 min. Measurements were conducted using a Luminoskan™ Microplate Luminometer. The EC_{50} and EC_{20} (concentration that provoked 50% and 20% of bioluminescence inhibition, respectively) were calculated using the parameters provided by the Ascent Software by Aboatox Co. (Finland). Finally, the EC_{50} values were used to calculate toxicity units (TU) as $100/EC_{50}$. TU are classified into four distinct groups: non-toxic ($TU < 1$), toxic ($1 < TU < 10$), very toxic ($10 < TU < 100$) and extremely toxic ($TU > 100$). Further details on the methodology can be found in Kováts et al. (2012) and Vicente et al. (2021). The bioassay is a good indicator of the metabolic activity of an organism as bioluminescence is directly linked to respiratory activity. Being a direct contact test, it simulates a potentially realistic exposure route that occurs between the particles and the recipient biological systems. In addition, it is reproducible, and, contrary to other toxicological tests, the bulk samples are assayed without prior extraction, and no organic solvents are used.

2.7 Emission Factors

To roughly estimate PM_{10} emission factors (EF) from road dust resuspension, the empirical relationship proposed by Amato et al. (2011) was employed:

$$EF = 45.9 \times DL^{0.81} \tag{1}$$

where EF expresses the PM_{10} emission factor (milligrams per vehicle and kilometer travelled, mg veh^{-1} km^{-1}) and DL refers to the road dust loadings (mg m^{-2}) obtained at each sampling site.

2.8 Contaminant Level Assessment

2.8.1 Geo-accumulation Index

The geo-accumulation index (I_{geo}) was introduced by Muller (1979) as an indicator of anthropogenic pollution. I_{geo} is mathematically expressed as:

$$I_{geo} = \log_2\left(\frac{C_n}{1.5 \times B_n}\right) \tag{2}$$

where C_n represents the concentration of an element in road dust, and B_n is the geochemical background value. The B_n values were taken from Wedepohl (1995), since there are no geochemical background values for soils in the region. The factor of 1.5 incorporates possible variations in background data due to lithogenic effects. The I_{geo} scale consists of seven classes, ranging from uncontaminated to extremely contaminated, as follows: class 0, uncontaminated ($I_{geo} < 0$); class 1, uncontaminated to moderately contaminated ($0 \le I_{geo} < 1$); class 2, moderately contaminated ($1 \le I_{geo} < 2$); class 3, moderately to heavily contaminated ($2 \le I_{geo} < 3$); class 4, heavily contaminated ($3 \le I_{geo} < 4$); class 5, heavily to extremely contaminated ($4 \le I_{geo} < 5$); and class 6, extremely contaminated ($I_{geo} \ge 5$).

2.9 Enrichment Factor

Enrichment factors (EnF) have been extensively used to identify the contribution of anthropogenic and natural sources to individual elements of PM_{10} (Almeida-Silva et al., 2020; Gao et al., 2023; Pio et al., 2022; Uzoekwe et al., 2021). This index is based on the relationship between the concentration of an element (Ce) with the crustal concentration of a reference element (Cr). Due to the abundant natural occurrence on Earth's crust, Al was selected for this study as a reference element. EnF was calculated as follows:

$$EnF = \frac{\frac{Ce}{Cr}\left(PM_{10}sample\right)}{\frac{Ce}{Cr}(Crustal)} \tag{3}$$

As stated before, due to the unavailability of compositional values for the local soil, the Earth's crust individual elemental composition was taken from Wedepohl (1995). Five categories were considered: EnF < 2 minimal enrichment; 2 ≥ EnF < 5 moderate enrichment; 5 ≥ EnF < 20 significant enrichment; 20 ≥ EnF < 40 very high enrichment; and EnF ≥ 40 extremely high enrichment (Yang et al., 2016).

2.10 Health Risk of Exposure to Potential Toxic Road Dust Elements

To evaluate the potential effects of toxic elements in road dust that residents can be directly exposed to, a human health risk assessment was carried out. Three main intake pathways were considered: inhalation of particles (oral and nasal intake), dermal absorption and ingestion (hand-to-mouth intake). For road dust, it was assumed that intake rates and particle emission are similar to those established for soils. The chronic daily intake (CDI_{route}, ingestion (ing) and dermal absorption (drm) in mg $kg^{-1} \cdot d^{-1}$; inhalation (inh) of particles in mg m^{-3} for non-carcinogenic effects, and μg m^{-3} for carcinogenic effects), was calculated for each exposure route and for individual elements:

$$CDI_{ing} = \frac{C \times IngR \times EFreq \times ED}{BW \times AT} \times 10^{-6} \tag{4}$$

$$CDI_{drm} = \frac{C \times SA \times SAF \times DA \times EFreq \times ED}{BW \times AT} \times 10^{-6} \tag{5}$$

$$CDI_{inh} = \frac{C \times InhR \times EFreq \times ED}{BW \times AT \times PEF} \tag{6}$$

where C is the element concentration in road dust (mg kg^{-1}), IngR is the ingestion rate (200 and 100 mg d^{-1} for children and adults, respectively), InhR is the inhalation rate (7.6 and 20 m^3 d^{-1} for children and adults, respectively), EF is the exposure frequency (180 d yr^{-1}), ED is the exposure duration (6 and

24 years for non-carcinogenic effects in children and adults, respectively, and 70 years is the lifetime for carcinogenic effects), BW is the average body weight (15 and 70 kg for children and adults, respectively), AT is the averaging time for non-carcinogenic effects (AT days = ED × 365), SA is the exposed skin area (2800 and 5700 cm^2 for children and adults, respectively), SAF is the skin adherence factor (0.2 and 0.07 mg cm^{-2} for children and adults, respectively), DA is the dermal absorption factor (0.03 for As and 0.001 for other elements), and PEF is the particulate emission factor (1.36×10^9 m^3 kg^{-1}) (USEPA, 2010). In CDI_{ing} and CDI_{drm}, 10^{-6} is a conversion factor (kg mg^{-1}). For each element and route, the chronic hazard quotient (HQ) was estimated for non-cancer toxic risks, with R_fD being the chronic reference dose:

$$HQ_{route} = \frac{CDI_{route}}{RfD_{route}} \tag{7}$$

$$HI = HQ_{ing} + HQ_{drm} + HQ_{inh} \tag{8}$$

An HQ (dimensionless) less than 1 indicates that adverse effects are not likely to occur, whereas values higher than 1 suggest that there is a high probability of potential health risks may occur with overexposure. The sum of HQ for each pathway was performed to calculate the cumulative non-carcinogenic hazard index (HI), assuming that risks are additive. The assessment of non-carcinogenic risks associated with exposure to PM_{10}-bound elements has been widely performed in road dust studies (Candeias et al., 2020; Faisal et al., 2021; Li et al., 2018; Shahab et al., 2020).

To evaluate the carcinogenic risk (CR) for specific metals, the following equation was applied:

$$CR = CDI \times SF \tag{9}$$

where SF is the slope factor for carcinogenic metals: Cr (42 mg kg^{-1} $day^{-1)}$, Ni (0.84 mg kg^{-1} day^{-1}), Cd (6.3 mg kg^{-1} day^{-1}), and Co (9.8 mg kg^{-1} day^{-1}) (USEPA, 2010). The total carcinogenic risk (TCR) is represented by the sum of CR values for each metal and is a dimensionless value. According to USEPA (2010), values of $10^{-6} \geq TCR \leq 10^{-4}$ are considered acceptable or tolerable risks, values lower than 10^{-6} represent no significant health hazard and values higher than 10^{-4} indicate unacceptable risks. The values of SF were only available for inhalation, so the cancer risk for ingestion and dermal pathways could not be estimated.

2.11 Data Analysis

Statistical analysis was done using the IBM SPSS software (version 25). Graphs and maps were created using Matlab (version R2019a) and ArcGis (version 10.6.1), respectively. Nonparametric tests, namely Mann–Whitney and Spearman, were applied to evaluate statistical differences between samples and the correlation between elements, respectively, at a confidence level of 95% ($p < 0.05$). Hierarchical cluster analyses (HCA) was used to reveal similarities between road dust sampling sites in the study area. To perform HCA, the Ward's method and the Euclidean distance were used. To illustrate the possible relationships among the sampling sites the results were reported in the form of a dendrogram.

3 Results and Discussion

3.1 PM_{10} Road Dust Loadings and Emission Factors

Road dust loadings in Bragança were lower than those documented for other European cities. Loadings ranging from 0.02 to 0.15 mg PM_{10} m^{-2} were obtained (Fig. 3), while a mean value significantly higher (4.40 mg PM_{10} m^{-2}) was found in Lisbon (Cunha-Lopes et al., 2022). In Aveiro, Portugal, mass loadings ranged between 0.33 and 6.57 mg PM_{10} m^{-2} (Casotti Rienda et al., 2023b), with the highest values recorded at a trafficked roundabout. Mean values for typical inner-city roads in Paris were in the range 0.7–2.2 mg PM_{10} m^{-2}, similarly to loadings observed in the Portuguese cities of Viana do Castelo and Oporto, but lower than those in Spain (Alves et al., 2018, 2020; Amato et al., 2009). The variability of DL within cities demonstrates the high dependence on the local features, especially the road characteristics and type of pavement, traffic conditions, handling of dusty materials, land use and (Amato et al., 2009; Han et al., 2007; Zhao et al., 2006). On the other hand, as demonstrated by Casotti Rienda and Alves (2021), different sampling strategies can lead to discrepancies in the values obtained.

The variability of DL between sampling sites was significant, but some general patterns were identified.

Fig. 3 Spatial distribution of PM_{10} emission factors (**a**) and dust loadings (**b**)

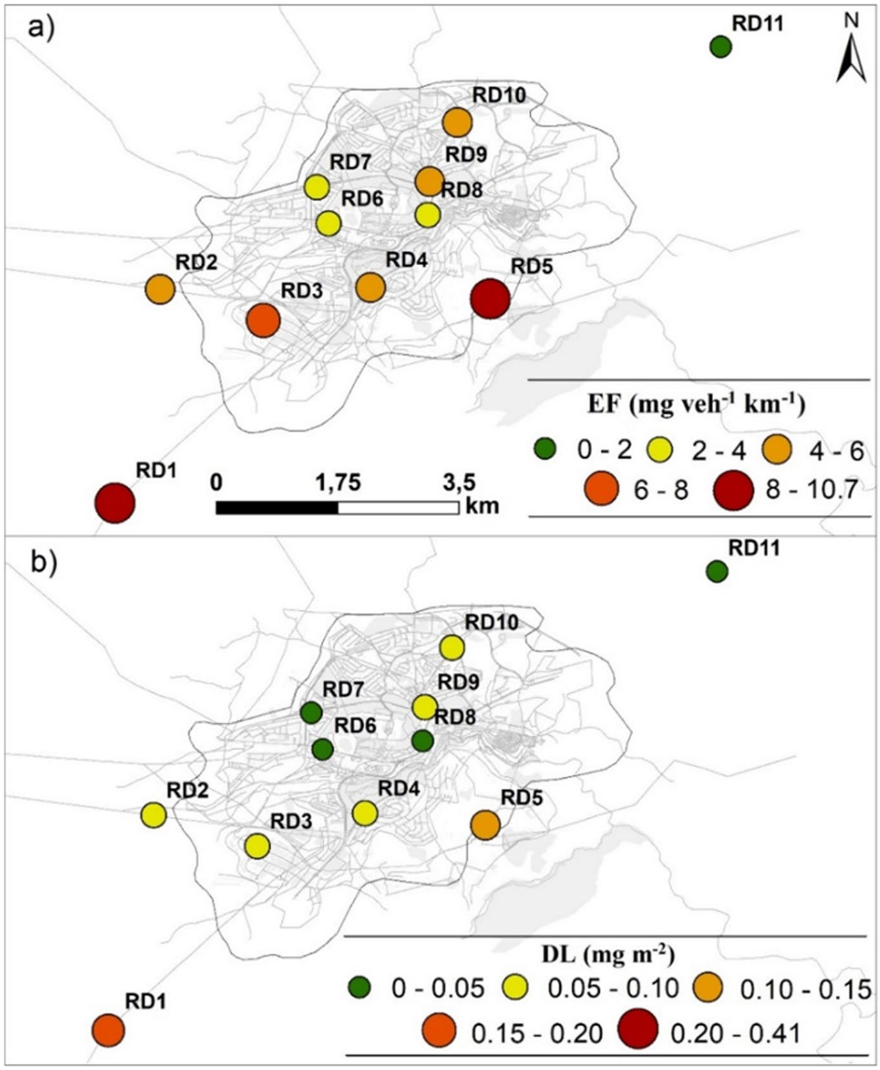

Higher dust loadings (DL > 0.15 mg PM_{10} m^{-2}) were observed in the surrounding areas of the city, with RD1 and RD5 affected by the evident wear of the asphalt and most likely by agricultural activities. As described for cobblestone pavements (Alves et al., 2018, 2020), asphalt-paved roads in poor conditions can favour wear processes because of the strong interaction between the pavement and the tyres, as well as the deposit of particulate material in the cracks, leading to higher resuspension dust loads. Lower dust loadings were obtained for samples taken within the residential area, where routine maintenance of the pavement and low traffic density are registered.

Emission factors ranged between 2.16 and 10.1 mg veh^{-1} km^{-1}. The values are lower than EFs of 14–23 mg veh^{-1} km^{-1} reported for a mixed fleet in the UK (Thorpe et al., 2007), 12.0 to 29.4 mg veh^{-1} km^{-1} derived for asphalt roads in Oporto (Alves et al., 2018), 27.0 mg veh^{-1} km^{-1} in Turin (Padoan & Amato, 2018) or 24 mg km^{-1} veh^{-1} in Milan (Amato et al., 2017). It should be noted, however, that comparisons should be seen as indicative. The EFs, in addition to representing realities with different circulation patterns, can vary depending on the sampling methodology used.

3.2 PM_{10} Carbonaceous and Elemental Composition

OC could not be separated from EC in most samples (> 80%), due to the low laser performance. The laser was disturbed by the presence of iron oxides in the samples, compromising the correct separation between OC and EC (Kau et al., 2022). Thus, the carbonaceous content is presented as total carbon (TC = OC + EC). TC accounted for 14.9 ± 6.8% (133 ± 72.0 mg g^{-1}) of the total mass concentrations, ranging between 8 and 32% of PM_{10}. Similar values of TC/PM_{10} were obtained for other urban centres (Table 1). In Raipur, lower percentages (2.3 ± 7.2%) were reported for the thoracic fraction of resuspended road dust (Giri et al., 2013). The TC content decreased from roads near construction sites in the city centre (150 – 303 mg g^{-1}) to suburban areas (18 – 105 mg g^{-1}).

Elements represented the largest share of PM_{10}. The major PM_{10}-bound elements were Si (15.4%), Ca (5.5%), Al (5.1%), Fe (4.0%) and Mg (2.9%), while the most abundant trace elements were Cu, Zn, and Ba, followed by Cr, Ni and Pb (Table 2).

To perform a PM_{10} mass balance, major and trace element concentrations were converted into the equivalent oxide species (SiO_2, CaO, Al_2O_3, Fe_2O_3, etc.) and summed. SiO_2 was estimated as $3 \times Al_2O_3$ (Brines et al., 2016). Element oxides accounted for a PM_{10} mass fraction of 28.6 ± 18.7%, varying from 8 to 15% near residential areas, 27% in the industrial area, 24–29% on streets with more intense traffic, and 20–85% in suburban areas. The average percentage was very close to the 29 ± 7.5% found in Oporto (Alves et al., 2018) and 16.9–28.1% in Lisbon (Cunha-Lopes et al., 2022), but is lower than the 61.4 ± 8.6% of Aveiro (Casotti Rienda et al., 2023b) and 70% of Viana do Castelo (Alves et al., 2020). The higher values could be associated with the poor state of the pavement, dust contribution from construction works and emissions from specific sources (e.g., quarries, cement plants).

Specific element ratios were often used as diagnostic tools that can help identify emitting sources (Pant et al., 2015; Pio et al., 2022; Querol et al., 2007). A compilation of values is provided in Table 3. In the present study, the Cu/Pb and Zn/Pb ratios were up to 9 times higher than the values reported for road dust samples of other regions, approaching the typical ratios for brake dust. The Fe/Al (1.83) was higher than the ratio in the upper Earth's crust (0.40), possibly due to the emission of Fe from traffic-related sources. K/Al and Ti/Al ratios showed insignificant variations between sites, with values similar to those reported for the upper Earth's crust (0.37 K/Al and 0.04 Ti/Al). This points to a geogenic origin of these elements, similar to what was observed in cities such as Barcelona and Aveiro.

The Ca/Al ratio varied from 0.78 up to 5. The highest values were observed for roads near construction sites. Ca/Al ratios in samples from streets RD6, RD9 and RD11 were 4.2, 5.0 and 4.8, respectively. These results are in line with values previously reported of 4.04 for Fushun (Kong et al., 2011) and 3.60 (Amato et al., 2009) for a construction area in Barcelona. Furthermore, Ca/Al can be an indicator of abrasion-led resuspension processes. The PM_{10} ratio of Cu/Zn (2.29) in this study was higher than those documented for road dust samples from other cities (0.27–0.90), light-duty diesel vehicles (0.14), and fugitive dust (0.17), but was quite similar to the ratio reported for brake dust (2.38), indicating that Cu, Zn and Pb were mainly derived from this source.

3.3 Pollution Indexes

To assess the intensity of road dust contamination by anthropogenic sources, enrichment factors (EnFs) were calculated for PM_{10}-bound elements. The elements with minimal to moderate

Table 1 Comparison of OC/EC ratios and carbonaceous content of PM_{10} from road dust resuspension of the present study and values reported in the literature

		OC/EC	OC/PM_{10} (wt%)	TC/PM_{10} /wt%)
This study	Bragança (Portugal)	-	-	14.9 ± 6.8
Casotti Rienda et al. (2023b)	Aveiro (Portugal)	1.89–4.03	13.4 ± 1.4	19.8 ± 2.05
Cunha-Lopes et al. (2022)	Lisbon (Portugal)	0.60–5.33	10.4 ± 0.03	11.9 ± 23.2
Ramírez et al. (2019)	Bogotá (Colombia)	10.0–36.3	13–29	-
Amato et al. (2009)	Barcelona (Spain)	3.00–4.90	11.7 ± 1.8	-

Table 2 Descriptive statistics of mass fractions of PM_{10}-bound chemical constituents in road dust (min, max and mean ± SD)

$\mu g\ g^{-1}$	min	max	mean ± SD
Li	1.20	42.7	23.2 ± 13.5
Sc	2.90	10.8	7.12 ± 2.90
V	3.80	145	56.4 ± 44.3
Cr	24.2	234	152 ± 72.3
Co	2.60	32.6	15.4 ± 11.5
Ni	1.80	350	166 ± 98.7
Cu	1175	13339	4611 ± 3759
Zn	1187	5305	2466 ± 1163
Ga	6.40	14.4	9.45 ± 2.93
Se	0.30	0.80	0.61 ± 0.23
Rb	10.8	99.9	51.9 ± 28.4
Sr	20.0	217	77.9 ± 50.2
Y	0.30	19.7	8.27 ± 6.01
Zr	5.50	99.4	36.9 ± 27.9
Nb	0.30	0.30	0.31 ± 0.15
Cd	0.30	10.8	3.87 ± 5.06
Sn	2.30	122	26.6 ± 32.6
Cs	1.60	3.80	3.09 ± 0.92
Ba	73.7	730	379 ± 192
La	0.00	17.1	8.44 ± 6.54
Ce	4.80	38.3	22.6 ± 11.5
Pr	0.00	1.30	0.61 ± 0.50
Nd	0.30	15.4	8.13 ± 5.92
Sm	0.30	0.40	0.48 ± 0.12
Gd	0.10	1.10	0.61 ± 0.42
Dy	0.10	0.10	0.13 ± 0.10
Pb	19.8	437	113 ± 112
Bi	1.30	1.30	1.35 ± 0.15
Th	0.40	3.20	2.14 ± 1.18
U	1.10	5.50	2.77 ± 2.02
$mg\ g^{-1}$			
Total Carbon (TC)	18.7	303	133 ± 72.0
Al	4.00	63.2	27.1 ± 17.5
Ca	13.8	136	39.5 ± 32.3
Fe	9.50	49.5	30.8 ± 11.9
K	0.90	15.8	6.10 ± 5.23
Mg	6.00	35.3	17.3 ± 8.02
Mn	0.60	1.42	1.01 ± 0.35
Na	0.60	14.6	5.52 ± 4.12
P	0.70	23.8	4.73 ± 7.81
S	3.40	23.4	8.81 ± 6.48
Ti	0.90	4.92	2.78 ± 1.23
Si	0.70	94.8	33.1 ± 31.9

enrichments (EnF < 5) were Si, Al, K, Fe, Mg, Mn, Na, Ti, Li, Sc, V, Ga, Rb, Sr, Y, Zr, Nb, Cd, Sn, Cs, Ba, La, Ce, Pr, Nd, Sm, Eu, Gd, Tb, Dy, Tl, Bi, Th and U, indicating a major natural geogenic origin. Cu showed the highest EnF (2710), followed by Zn (260), S (74), Pb (43) and Ni (40), classified as extremely high enrichments. Furthermore, significant enrichments were estimated for Cr (19), Co (9), Ca (5), and P (9), indicating that these elements could be linked with anthropogenic sources. A previous study using receptor modelling to apportion sources of ambient PM_{10} in Bragança (Cipoli et al., 2023) during the winter season has also shown high enrichments for some of these elements, especially for Br (449), Zn (93), Cu (72) and Pb (65), pointing to the contribution of anthropogenic sources, both for PM_{10} in the air and for PM_{10} resuspended from dust deposited on roads. Cu is commonly present in particles from brake wear, tyre wear and brake linings (El-Fadel & Hashisho, 2001). Cu showed statistically significant correlations with Pb (R = 0.71), S (R = 0.91), Ti (0.66) and Mn (0.63), suggesting similar emission sources. Although Europe phased-out leaded gasoline, there may be a lot of Pb accumulated in road dust instead related to other vehicle emissions, especially from tyre and brake wear, and from engine oil impurities (Alves et al., 2020; Panko et al., 2018). In addition to other traffic-related emissions, Zn is widely used in the galvanising process of tyres (Jeong, 2022), while S is a typical component of lubricant oils and brake pads (Sathickbasha et al., 2019). In general, the highest enrichments were found inside the tunnel, where vehicle emissions dominate and the dispersion of pollutants is more limited. However, moderately to extremely enrichments were found for S, Cu, Pb and Zn in suburban areas, which are influenced by agricultural activities, including soil preparation, sowing, cultivation, fertilizer application, as well as the use of fossil fuel-powered machinery.

As pointed out by the enrichment factors, the Igeo values revealed that road dust of Bragança is heavily to extremely contaminated by elements from traffic, such as Ni, Zn and Cu, whose concentrations were well above the natural background. Moderate contamination was also noticed for Cr, Sn, and Pb. All other elements presented Igeo < 0.

Table 3 Ratios between elements in PM_{10} from different studies

		Fe/Al	K/Al	Ca/Al	Ti/Al	Fe/Cu	Cu/Zn	Cu/Pb	Zn/Pb
Our study	Urban road dust (Bragança)	1.83	0.32	2.15	0.07	10.5	2.29	60.8	35.3
(Alves et al., 2020)	Urban road dust (Viana do Castelo)	0.96	0.27	0.51	0.10	35.1	0.84	6.58	7.83
(Casotti Rienda et al., 2023b)	Urban road dust (Aveiro)	1.00	0.35	2.49	0.06	50.6	0.50	-	-
(Ramírez et al., 2019)	Residential road dust (Bogota)	0.41	0.11	0.95	0.06	-	0.25	1.09	4.38
(Amato et al., 2009)	Urban road dust (Barcelona)	1.21	0.33	3.05	0.07	52.1	0.90	6.18	6.81
(Zhang et al., 2018)	Roadside microenvironments (China)	0.71	0.21	0.86	0.05	102.8	0.27	1.23	4.45
(Hulskotte et al., 2014)	Brake dust (Netherlands)	13.3	-	-	0.53	2.03	2.38	85.8	36.0
(Chiang et al., 2012)	Ligh-duty diesel (China)	0.6	0.46	0.71	-	16.2	0.14	0.29	2.13
(Kong et al., 2011)	Fugitive dust (China)	0.15	0.03	1.29	0.06	71.0	0.17	1.93	11.1

3.4 Cluster Analysis

Based on the road dust PM_{10}-bound elements of the diverse sampling sites, five clusters were established (Fig. 4). RD4, RD8, RD9 and RD6 were grouped in cluster 1 (CA1), with abundant PM_{10} mass fractions of Cr, Cu, Zn, Ba and Pb, which were related to traffic (Amato et al., 2016). Moreover, RD4 and RD8, both located in avenues with medium–high traffic density during peak hours (Cipoli et al., 2022), showed the highest similarity. CA2 is composed of RD7 and RD11, for which the sum of element oxides comprised the lowest contribution to the PM_{10} mass, with 8% and 15%, respectively.

CA3 comprised the suburban samples RD2, RD10 and, which were enriched in Al, Ca, Fe, Mg, Ni and Cr, reflecting the presence of mineral dust from soil mixed with some anthropogenic elements. RD5 (cluster 4) and RD1 (cluster 5) presented the highest dissimilarities. Interestingly, concentrations of specific elements, such as Se, Cd, Sm, Gd and U, were only detected in these locations, possibly due to the proximity of agricultural activities. Furthermore, RD1 presented the highest concentrations of PM_{10}-bound elements, accounting for 85% of the PM_{10} mass. While RD1 was more impacted by agricultural activities, RD5 had the most deteriorated pavement of all sampling sites. To correctly examine whether the Euclidean distances to the original unmodeled data pairs are correct to the dendrogram, the cophonetic correlation coefficient was calculated, in which values close to 1 reflects that the clustering solution is accurately. In this study the coefficient was 0.92, reflecting a good precision in cluster pairs.

Fig. 4 Dendrogram of the cluster analysis for PM_{10} road dust sampling sites

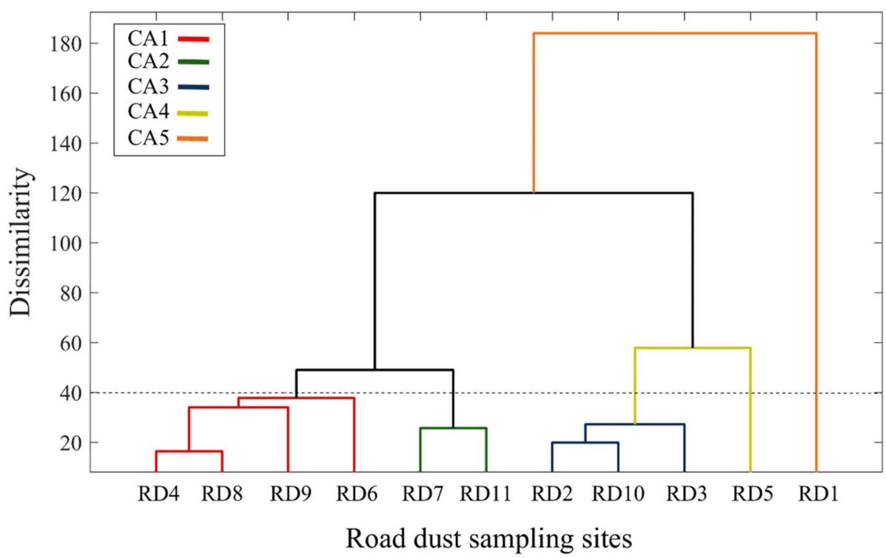

3.5 Ecotoxicity

The bioluminescence inhibition bioassay with *Allivibrio fisheri* has been previously applied to PM_{10} from road dust resuspension of other cities in Portugal (Casotti Rienda et al., 2023a, 2023b). In this study, TU ranged between 1.92 and 3.9, indicating that all samples proved to be toxic. The highest TU (RD5 3.90, RD6 3.53 and RD7 3.31) values were observed for samples with higher carbonaceous content. Available literature indeed shows that the carbonaceous content in ambient PM contributes significantly to aerosol toxicity (Kováts et al., 2021; Vicente et al., 2021). Furthermore, toxicity levels may not only be related to high PM_{10} concentrations, but mainly to specific PM_{10}-bound constituents that are known to have deleterious effects, such as PAHs or some elements (Lee et al., 2003; Romano et al., 2020). A clear negative correlation between some specific PM_{10}-bound elements and EC_{50} have been reported (Casotti Rienda et al., 2023a; Kováts & Horváth, 2016; Romano et al., 2020). In this study, TU was inversely correlated with Cu ($r^2 = 0.79$), Pb ($r^2 = 0.80$) and S ($r^2 = 0.75$), indicating that an increased proportion of these elements leads to a lower amount of PM_{10} to induce a toxicological effect. Previous results of the *Allivibrio* assay have already proven sensitivity to Cu (Kováts et al., 2022).

3.6 Assessment of Potential Risks to Human Health

HI showed that the ingestion pathway of road dust particles appears to be the route of higher risk for all elements, followed by the dermal and inhalation routes (Table S1). However, the particle emission factor used to estimate the chronic daily dose by inhalation was developed for contaminated background soil, thus the results may be underestimated for concentrations of trace elements on road dust samples. For all elements, HI (sum of the three exposure pathways) was lower than the safe value of 1 for both adults and children, suggesting that the risk of developing non-cancer diseases in the population as a result of exposure to PM_{10} from road dust resuspension is low and acceptable. The values for children were found to be, on average, 54% higher than those for adults, showing the susceptibility of children to the health effects from metal(loid)s in road dust. The highest values were found for Fe (adult 0.12; children 0.22), Cr (adult 0.26; children 0.32) and Cu (adult 0.35; children 0.58).

The carcinogenic risk associated with Cr, Ni, Cd and Co was assessed for the inhalation route. The total carcinogenic risk (TCR) for adults and children was 9.02×10^{-7} and 1.88×10^{-6} (Table S2), respectively. These results represent no significant health hazard for adults and acceptable or tolerable risks for children, but in general, the total cancer risk can be considered insignificant for the population. Once again, the higher TCR values for children reflect that they are a more susceptible group to air pollution exposure (Bateson & Schwartz, 2007; Prunicki et al., 2021; Samoli et al., 2016).

4 Conclusions

For the first time, ecotoxicity, loadings and chemical patterns of the thoracic fraction of road dust (PM_{10}) were investigated in a small north-eastern city in Portugal, including industrial, suburban, and urban contexts. Data obtained locally is useful for completing emission inventories and can contribute as input values for receptor modelling methodologies. It is worth noting that the findings of this study are representative of the warm season in Bragança. The emissions factors obtained are lower than those reported in other cities, especially in medium-large urban centres such as Lisbon, Barcelona, Milan, Oporto, Viana do Castelo, or even Bogota. Although a different sampling approach has been adopted, the results obtained are in line with the spatial distribution and relationships between chemical constituents found in other studies, confirming the hypotheses that, in addition to vehicle density, the condition of the pavement and activities in the surrounding areas are major factors for dust loadings. The suburban context, with the presence of agricultural activities combined with degraded pavement, showed favourable conditions for accumulation and wear mechanisms leading to higher dust loadings.

Highly enriched elements such as Cu, Zn, S, Pb and Ni, especially in urban areas with a higher density of vehicles, suggested strong contributions from traffic-related sources. Nonetheless, in the suburban areas, alongside with a steady contribution of crustal elements, moderately to extremely enriched metal(loid)s were observed, such as S, Cu, Pb and Zn, linked to agricultural activities. Furthermore, the geochemical indices showed that road dust of the study region is extremely contaminated by elements mainly originated from tyre and brake wear (Ni, Zn and Cu), especially in the samples collected inside the tunnel. Thus, non-exhaust emissions represent a noteworthy contribution to the PM_{10} from road dust resuspension in Bragança, and together with other emissions sources may pose a significant ecological risk.

Although total non-carcinogenic and carcinogenic risks were found to be low for both children and adults, the bioluminescence inhibition assay showed (eco)toxic responses for all samples. Findings of this study indicate that hazards of exposure to road dust cannot be overlooked and further investigations with more detailed information are needed. Additional chemical constituents, such as PAHs, should be analysed to evaluate health risks more accurately. With the increase of government incentives for the acquisition of electric vehicles, an intensification of this new vehicle fleet in urban centers is to be expected in the coming decades. With different characteristics, especially higher weight, significant changes in suspended dust loads can occur, and for that, further investigations to provide realistic information and preventive and corrective actions should be targeted.

Acknowledgements Yago A. Cipoli acknowledges the Portuguese Foundation for Science and Technology (FCT) for the PhD scholarship (SFRH/BD/04992/2021). The authors are grateful to FCT for its financial support through national funds FCT/MCTES (PIDDAC) to CIMO (UIDB/00690/2020 and UIDP/00690/2020), SusTEC (LA/P/0007/2020) and CESAM (UIDP/50017/2020, UIDB/50017/2020 and LAP/0094/2020). The research work was also supported by the Municipality of Bragança. We thank the authorities for their support in carrying out the sampling tasks.

Authors' Contribution Yago A. Cipoli: Conceptualisation, Formal analysis, Investigation, Methodology, Writing – original draft & Editing. Ismael C. Rienda: Methodology. Ana M. S. de la Campa: Methodology. Nora Kováts: Methodology. Teresa Nunes: Methodology. Manuel Feliciano: Supervision, Writing—Review & Editing. András Hoffer: Methodology. Beatrix Jancsek-Turóczi: Methodology. Célia Alves: Writing original draft and review, Conceptualisation, Methodology, Supervision, Funding acquisition.

Funding Open access funding provided by FCT|FCCN (b-on).

Data Availability The data that support the fndings of this study are available from the corresponding author upon reasonable request.

Declarations

Competing Interest The authors declare that they have no known competing financial interests or personal relationships that could have appeared to influence the work reported in this paper.

References

Almeida-Silva, M., Canha, N., Vogado, F., Baptista, P. C., Faria, A. V., Faria, T., et al. (2020). Assessment of particulate matter levels and sources in a street canyon at Loures, Portugal – A case study of the REMEDIO project. *Atmospheric Pollution Research, 11*(10), 1857–1869. https://doi.org/10.1016/J.APR.2020.07.021

Alves, C., Gonçalves, C., Fernandes, A. P., Tarelho, L., & Pio, C. (2011). Fireplace and woodstove fine particle emissions from combustion of western Mediterranean wood types. *Atmospheric Research, 101*(3), 692–700. https://doi.org/10.1016/J.ATMOSRES.2011.04.015

Alves, C. A., Evtyugina, M., Vicente, A. M. P., Vicente, E. D., Nunes, T. V., Silva, P. M. A., et al. (2018). Chemical profiling of PM_{10} from urban road dust. *Science of the Total Environment, 634*, 41–51. https://doi.org/10.1016/J.SCITOTENV.2018.03.338

Alves, C. A., Vicente, E. D., Vicente, A. M. P., Rienda, I. C., Tomé, M., Querol, X., & Amato, F. (2020). Loadings, chemical patterns and risks of inhalable road dust particles in an Atlantic city in the north of Portugal. *Science of the Total Environment, 737*, 139596. https://doi.org/10.1016/J.SCITOTENV.2020.139596

Amato, F., Pandolfi, M., Viana, M., Querol, X., Alastuey, A., & Moreno, T. (2009). Spatial and chemical patterns of PM_{10} in road dust deposited in urban environment. *Atmospheric Environment, 43*(9), 1650–1659. https://doi.org/10.1016/J.ATMOSENV.2008.12.009

Amato, F., Pandolfi, M., Moreno, T., Furger, M., Pey, J., Alastuey, A., et al. (2011). Sources and variability of inhalable road dust particles in three European cities. *Atmospheric Environment, 45*(37), 6777–6787. https://doi.org/10.1016/J.ATMOSENV.2011.06.003

Amato, F., Favez, O., Pandolfi, M., Alastuey, A., Querol, X., Moukhtar, S., et al. (2016). Traffic induced particle resuspension in Paris: Emission factors and source contributions. *Atmospheric Environment, 129*, 114–124. https://doi.org/10.1016/J.ATMOSENV.2016.01.022

Amato, F., Bedogni, M., Padoan, E., Querol, X., Ealo, M., & Rivas, I. (2017). Characterization of road dust emissions in milan: Impact of vehicle fleet speed. *Aerosol and Air Quality Research, 17*(10), 2438–2449. https://doi.org/10.4209/AAQR.2017.01.0017

Apte, J. S., Brauer, M., Cohen, A. J., Ezzati, M., & Pope, C. A. (2018). Ambient $PM_{2.5}$ reduces global and regional life expectancy. *Environmental Science and Technology Letters, 5*(9), 546–551. https://doi.org/10.1021/ACS.ESTLETT.8B00360

Bateson, T. F., & Schwartz, J. (2007). Children's response to air pollutants. *Journal of Toxicology and Environmental Health, Part A, 71*(3), 238–243. https://doi.org/10.1080/15287390701598234

Brines, M., Dall'Osto, M., Amato, F., Minguillón, M. C., Karanasiou, A., Alastuey, A., & Querol, X. (2016). Vertical and horizontal variability of PM_{10} source contributions in Barcelona during SAPUSS. *Atmospheric Chemistry and Physics, 16*(11), 6785–6804. https://doi.org/10.5194/ACP-16-6785-2016

Candeias, C., Vicente, E., Tomé, M., Rocha, F., Ávila, P., & Alves, C. (2020). Geochemical, mineralogical and morphological characterisation of road dust and associated health risks. *International Journal of Environmental Research and Public Health, 17*(5), 1563. https://doi.org/10.3390/IJERPH17051563

Casotti Rienda, I., & Alves, C. A. (2021). Road dust resuspension: A review. *Atmospheric Research, 261*, 105740. https://doi.org/10.1016/J.ATMOSRES.2021.105740

Casotti Rienda, I., Alves, C. A., Nunes, T., Soares, M., Amato, F., Sánchez de la Campa, A., et al. (2023a). PM_{10} Resuspension of road dust in different types of parking lots: Emissions, chemical characterisation and ecotoxicity. *Atmosphere, 14*(2), 305. https://doi.org/10.3390/ATMOS14020305

Casotti Rienda, I., Nunes, T., Gonçalves, C., Vicente, A., Amato, F., Lucarelli, F., et al. (2023b). Road dust resuspension in a coastal Atlantic intermunicipal urban area with industrial facilities: Emission factors, chemical composition and ecotoxicity. *Atmospheric Research, 294*, 106977. https://doi.org/10.1016/J.ATMOSRES.2023.106977

Chiang, H. L., Lai, Y. M., & Chang, S. Y. (2012). Pollutant constituents of exhaust emitted from light-duty diesel vehicles. *Atmospheric Environment, 47*, 399–406. https://doi.org/10.1016/J.ATMOSENV.2011.10.045

Cipoli, Y. A., Targino, A. C., Krecl, P., Furst, L. C., Alves, C. D. A., & Feliciano, M. (2022). Ambient concentrations and dosimetry of inhaled size-segregated particulate matter during periods of low urban mobility in Bragança. *Portugal. Atmospheric Pollution Research, 13*(9), 101512. https://doi.org/10.1016/J.APR.2022.101512

Cipoli, Y. A., Alves, C., Rapuano, M., Evtyugina, M., Rienda, I. C., Kováts, N., et al. (2023). Nighttime–daytime PM_{10} source apportionment and toxicity in a remoteness inland city of the Iberian Peninsula. *Atmospheric Environment, 303*, 119771. https://doi.org/10.1016/j.atmosenv.2023.119771

Cunha-Lopes, I., Alves, C. A., Casotti Rienda, I., Faria, T., Lucarelli, F., Querol, X., et al. (2022). Characterisation of non-exhaust emissions from road traffic in Lisbon. *Atmospheric Environment, 286*, 119221. https://doi.org/10.1016/J.ATMOSENV.2022.119221

Duan, R. R., Hao, K., & Yang, T. (2020). Air pollution and chronic obstructive pulmonary disease. *Chronic Diseases and Translational Medicine, 6*(4), 260–269. https://doi.org/10.1016/J.CDTM.2020.05.004

EEA. (2020). Air quality in Europe - 2020 report — European Environment Agency. https://www.eea.europa.eu/publications/air-quality-in-europe-2020-report. Accessed 01 July 202

El-Fadel, M., & Hashisho, Z. (2001). Vehicular emissions in roadway tunnels: A critical review. *Critical Reviews in Environmental Science and Technology, 31*(2), 125–174. https://doi.org/10.1080/20016491089190

Faisal, M., Wu, Z., Wang, H., Hussain, Z., & Azam, M. I. (2021). Human health risk assessment of heavy metals in the urban road dust of Zhengzhou metropolis, China. *Atmosphere, 12*(9), 1213. https://doi.org/10.3390/ATMOS12091213

FarwickZum Hagen, F. H., Mathissen, M., Grabiec, T., Hennicke, T., Rettig, M., Grochowicz, J., et al. (2019). On-road vehicle measurements of brake wear particle emissions. *Atmospheric Environment, 217*, 116943. https://doi.org/10.1016/J.ATMOSENV.2019.116943

Gao, Q., Zhu, S., Zhou, K., Zhai, J., Chen, S., Wang, Q., et al. (2023). High enrichment of heavy metals in fine particulate matter through dust aerosol generation. *Atmospheric Chemistry and Physics, 23*(20), 13049–13060. https://doi.org/10.5194/ACP-23-13049-2023

Giri, B., Patel, K. S., Jaiswal, N. K., Sharma, S., Ambade, B., Wang, W., et al. (2013). Composition and sources of organic tracers in aerosol particles of industrial central India. *Atmospheric Research, 120–121*, 312–324. https://doi.org/10.1016/J.ATMOSRES.2012.09.016

Gonçalves, A., Ornellas, G., Ribeiro, A. C., Maia, F., Rocha, A., & Feliciano, M. (2018). Urban cold and heat island in the city of Bragança (Portugal). *Climate, 6*(3), 70. https://doi.org/10.3390/CLI6030070

Gulia, S., Goyal, P., Goyal, S. K., & Kumar, R. (2019). Re-suspension of road dust: contribution, assessment and control through dust suppressants—a review. *International Journal of Environmental Science and Technology, 16*(3), 1717–1728.

Gustafsson, M., Blomqvist, G., Järlskog, I., Lundberg, J., Janhäll, S., Elmgren, M., et al. (2019). Road dust load dynamics and influencing factors for six winter seasons in Stockholm, Sweden. *Atmospheric Environment: X, 2*, 100014. https://doi.org/10.1016/J.AEAOA.2019.100014

Han, L., Zhuang, G., Cheng, S., Wang, Y., & Li, J. (2007). Characteristics of re-suspended road dust and its impact on the atmospheric environment in Beijing. *Atmospheric*

Environment, 41(35), 7485–7499. https://doi.org/10.1016/J.ATMOSENV.2007.05.044

Hans Wedepohl, K. (1995). The composition of the continental crust. *Geochimica Et Cosmochimica Acta, 59*(7), 1217–1232. https://doi.org/10.1016/0016-7037(95)00038-2

Harrison, R. M., Allan, J., Carruthers, D., Heal, M. R., Lewis, A. C., Marner, B., et al. (2021a). Non-exhaust vehicle emissions of particulate matter and VOC from road traffic: A review. *Atmospheric Environment, 262*, 118592. https://doi.org/10.1016/J.ATMOSENV.2021.118592

Harrison, R. M., Vu, T. V., Jafar, H., & Shi, Z. (2021b). More mileage in reducing urban air pollution from road traffic. *Environment International, 149*, 106329. https://doi.org/10.1016/J.ENVINT.2020.106329

Hicks, W., Beevers, S., Tremper, A. H., Stewart, G., Priestman, M., Kelly, F. J., et al. (2021). Quantification of non-exhaust particulate matter traffic emissions and the impact of COVID-19 lockdown at London Marylebone road. *Atmosphere, 12*(2), 190. https://doi.org/10.3390/ATMOS12020190

Hulskotte, J. H. J., Roskam, G. D., & Denier van der Gon, H. A. C. (2014). Elemental composition of current automotive braking materials and derived air emission factors. *Atmospheric Environment, 99*, 436–445. https://doi.org/10.1016/J.ATMOSENV.2014.10.007

Jancsek-Turóczi, B., Hoffer, A., Nyírö-Kósa, I., & Gelencsér, A. (2013). Sampling and characterization of resuspended and respirable road dust. *Journal of Aerosol Science, 65*, 69–76. https://doi.org/10.1016/J.JAEROSCI.2013.07.006

Jeong, H. (2022). Toxic metal concentrations and Cu–Zn–Pb isotopic compositions in tires. *Journal of Analytical Science and Technology, 13*(1), 1–10. https://doi.org/10.1186/S40543-021-00312-3

Kau, D., Greilinger, M., Kirchsteiger, B., Göndör, A., Herzig, C., Limbeck, A., et al. (2022). Thermal-optical analysis of quartz fiber filters loaded with snow samples-determination of iron based on interferences caused by mineral dust. *Atmospheric Measurement Techniques, 15*(18), 5207–5217. https://doi.org/10.5194/AMT-15-5207-2022

Kong, S., Ji, Y., Lu, B., Chen, L., Han, B., Li, Z., & Bai, Z. (2011). Characterization of PM10 source profiles for fugitive dust in Fushun-a city famous for coal. *Atmospheric Environment, 45*(30), 5351–5365. https://doi.org/10.1016/J.ATMOSENV.2011.06.050

Kováts, N., & Horváth, E. (2016). Bioluminescence-based assays for assessing eco- and genotoxicity of airborne emissions. *Luminescence, 31*(4), 918–923. https://doi.org/10.1002/BIO.3102

Kováts, N., Ács, A., Kovács, A., Ferincz, Á., Turóczi, B., & Gelencsér, A. (2012). Direct contact test for estimating the ecotoxicity of aerosol samples. *Environmental Toxicology and Pharmacology, 33*(2), 284–287. https://doi.org/10.1016/J.ETAP.2011.12.021

Kováts, N., Hubai, K., Sainnokhoi, T. A., Hoffer, A., & Teke, G. (2021). Ecotoxicity testing of airborne particulate matter—comparison of sample preparation techniques for the Vibrio fischeri assay. *Environmental Geochemistry and Health, 43*(11), 4367–4378. https://doi.org/10.1007/S10653-021-00927-W

Kováts, N., Hubai, K., Sainnokhoi, T. A., Eck-Varanka, B., Hoffer, A., Tóth, Á., et al. (2022). Ecotoxic emissions generated by illegal burning of household waste. *Chemosphere, 298*, 134263. https://doi.org/10.1016/J.CHEMOSPHERE.2022.134263

Lee, H. J., Villaume, J., Cullen, D. C., Kim, B. C., & Gu, M. B. (2003). Monitoring and classification of PAH toxicity using an immobilized bioluminescent bacteria. *Biosensors and Bioelectronics, 18*(5–6), 571–577. https://doi.org/10.1016/S0956-5663(03)00039-3

Lelieveld, J., Klingmü Ller, K., Pozzer, A., Pö Schl, U., Fnais, M., Daiber, A., & Mü Nzel, T. (2019). Cardiovascular disease burden from ambient air pollution in Europe reassessed using novel hazard ratio functions. *European Heart Journal, 40*, 1590–1596. https://doi.org/10.1093/eurheartj/ehz200

Li, N., Han, W., Tang, J., Bian, J., Sun, S., & Song, T. (2018). Pollution characteristics and human health risks of elements in road dust in Changchun, China. *International Journal of Environmental Research and Public Health, 15*(9), 1843. https://doi.org/10.3390/IJERPH15091843

Millán-Martínez, M., Sánchez-Rodas, D., de la Campa, A. M. S., & de la Rosa, J. (2021). Contribution of anthropogenic and natural sources in PM_{10} during North African dust events in Southern Europe. *Environmental Pollution, 290*, 118065. https://doi.org/10.1016/j.envpol.2021.118065

Muller, G. (1979). Schwermetalte in densdimenten des rheins veranderangen seit 1971. *Umschao, 79*(24), 778–783.

Padoan, E., & Amato, F. (2018). Vehicle non-exhaust emissions: impact on air quality. In *Non-Exhaust Emissions* (pp. 21–65). Academic Press. https://doi.org/10.1016/B978-0-12-811770-5.00002-9

Panko, J., Kreider, M., & Unice, K. (2018). Review of tire wear emissions: A review of tire emission measurement studies: identification of gaps and future needs. *Non-Exhaust Emissions*, 147–160. https://doi.org/10.1016/B978-0-12-811770-5.00007-8

Pant, P., Baker, S. J., Shukla, A., Maikawa, C., Godri Pollitt, K. J., & Harrison, R. M. (2015). The PM_{10} fraction of road dust in the UK and India: Characterization, source profiles and oxidative potential. *Science of the Total Environment, 530–531*, 445–452. https://doi.org/10.1016/J.SCITOTENV.2015.05.084

Pio, C., Cerqueira, M., Harrison, R. M., Nunes, T., Mirante, F., Alves, C., et al. (2011). OC/EC ratio observations in Europe: Re-thinking the approach for apportionment between primary and secondary organic carbon. *Atmospheric Environment, 45*(34), 6121–6132. https://doi.org/10.1016/J.ATMOSENV.2011.08.045

Pio, C., Rienda, I. C., Nunes, T., Gonçalves, C., Tchepel, O., Pina, N. K., et al. (2022). Impact of biomass burning and non-exhaust vehicle emissions on PM_{10} levels in a mid-size non-industrial western Iberian city. *Atmospheric Environment, 289*, 119293. https://doi.org/10.1016/J.ATMOSENV.2022.119293

Prunicki, M., Cauwenberghs, N., Lee, J., Zhou, X., Movassagh, H., Noth, E., et al. (2021). Air pollution exposure is linked with methylation of immunoregulatory genes, altered immune cell profiles, and increased blood pressure in children. *Scientific Reports, 11*(1), 1–12. https://doi.org/10.1038/s41598-021-83577-3

Querol, X., Viana, M., Alastuey, A., Amato, F., Moreno, T., Castillo, S., et al. (2007). Source origin of trace elements in PM from regional background, urban and industrial

sites of Spain. *Atmospheric Environment, 41*(34), 7219–7231. https://doi.org/10.1016/J.ATMOSENV.2007.05.022
Ramírez, O., Sánchez de la Campa, A. M., Amato, F., Moreno, T., Silva, L. F., & de la Rosa, J. D. (2019). Physicochemical characterization and sources of the thoracic fraction of road dust in a Latin American megacity. *Science of the Total Environment, 652*, 434–446. https://doi.org/10.1016/J.SCITOTENV.2018.10.214
Romano, S., Perrone, M. R., Becagli, S., Pietrogrande, M. C., Russo, M., Caricato, R., & Lionetto, M. G. (2020). Ecotoxicity, genotoxicity, and oxidative potential tests of atmospheric PM_{10} particles. *Atmospheric Environment, 221*, 117085. https://doi.org/10.1016/J.ATMOSENV.2019.117085
Samoli, E., Atkinson, R. W., Analitis, A., Fuller, G. W., Beddows, D., Green, D. C., et al. (2016). Differential health effects of short-term exposure to source-specific particles in London, U.K. *Environment International, 97*, 246–253. https://doi.org/10.1016/J.ENVINT.2016.09.017
Sathickbasha, K., Selvakumar, A. S., Balaji, M. A. S., & Rajan, B. S. (2019). The dual role of metal sulfides as lubricant and abrasive: an interface study in friction composite.https://doi.org/10.1088/2053-1591/aafd5a
Shaddick, G., Thomas, M. L., Mudu, P., Ruggeri, G., & Gumy, S. (2020). Half the world's population are exposed to increasing air pollution. *npj Climate and Atmospheric Science, 3*(1), 1–5. https://doi.org/10.1038/s41612-020-0124-2
Shahab, A., Zhang, H., Ullah, H., Rashid, A., Rad, S., Li, J., & Xiao, H. (2020). Pollution characteristics and toxicity of potentially toxic elements in road dust of a tourist city, Guilin, China: Ecological and health risk assessment. *Environmental Pollution, 266*, 115419. https://doi.org/10.1016/J.ENVPOL.2020.115419
Thorpe, A. J., Harrison, R. M., Boulter, P. G., & Mccrae, I. S. (2007). Estimation of particle resuspension source strength on a major London Road. *Atmospheric Environment, 41*, 8007–8020. https://doi.org/10.1016/j.atmosenv.2007.07.006
USEPA. (2010). *Regional screening levels for chemical contaminants at superfund sites*. Washington, DC: United States Environmental Protection Agency.
Uzoekwe, S. A., Izah, S. C., & Aigberua, A. O. (2021). Environmental and human health risk of heavy metals in atmospheric particulate matter (PM_{10}) around gas flaring vicinity in Bayelsa State, Nigeria. *Toxicology and Environmental Health Sciences, 13*(4), 323–335. https://doi.org/10.1007/S13530-021-00085-7
Vicente, E. D., Figueiredo, D., Gonçalves, C., Lopes, I., Oliveira, H., Kováts, N., et al. (2021). In vitro toxicity of indoor and outdoor PM_{10} from residential wood combustion. *Science of the Total Environment, 782*, 146820. https://doi.org/10.1016/J.SCITOTENV.2021.146820
Yang, X., Yan, J. I., Wang, F., Xu, J., Liu, X., Ma, K. E., et al. (2016). Comparison of organics and heavy metals acute toxicities to Vibrio fischeri. *Journal of the Serbian Chemical Society, 81*(6), 697–705. https://doi.org/10.2298/JSC151124011Y
Zhang, J., Wu, L., Fang, X., Li, F., Yang, Z., Wang, T., et al. (2018). Elemental composition and health risk assessment of PM_{10} and $PM_{2.5}$ in the roadside microenvironment in Tianjin, China. *Aerosol and Air Quality Research, 18*, 1817–1827. https://doi.org/10.4209/aaqr.2017.10.0383
Zhao, P., Feng, Y., Zhu, T., & Wu, J. (2006). Characterizations of resuspended dust in six cities of North China. *Atmospheric Environment, 40*(30), 5807–5814. https://doi.org/10.1016/J.ATMOSENV.2006.05.026